Journal of Materials Chemistry B

Accepted Manuscript

ROYAL SOCIETY OF CHEMISTRY

www.rsc.org/materialsB

conductivity of hemin.[18] So how to obtain the graphene with intrinsic peroxidase-like activity of hemin while simultaneously possessing excellent electron transfer ability for electrochemical sensing analysis is quite challenging.

Poly(3,4-ethylenedioxythiophene) (PEDOT) is one of the most popular conducting polymers in biosensors due to its excellent conductivity, good chemical stability and biocompatibility.[19] And unlike most thiophene derivatives, PEDOT can be polymerized in both organic and aqueous solutions,[20] so the synthesized PEDOT in aqueous solution enables its application in biosensors. Therefore, a bold idea that integrates H-GNs with PEDOT to form a novel sensing material comes to mind.

Herein, we introduce PEDOT conducting polymer into H-GNs to fabricate a novel H-GNs/PEDOT nanocomposite through simple microwave strategy. The conjugated hemin-graphene oxide acts as the initial precursor, in which graphene oxide is used as the oxidant of EDOT polymerization and hemin plays a role of a catalyst. Accurate detection of hydrogen peroxide (H_2O_2) is of important practical significance because it is an essential intermediate in food and pharmaceutical industrial production, clinic and environmental analyses.[21] On the basis of this nanocomposite, a biosensor for the quantitative determination of H_2O_2 is developed. Significantly, the H-GNs/PEDOT nanocomposite combines main excellent properties of graphene, hemin and PEDOT compositions. H-GNs/PEDOT not only maintains peroxidase-like activity of hemin that can catalyze the reduction of H_2O_2, but displays a high-speed electron transfer ascribed to the presence of PEDOT and graphene sheets. Furthermore, the sufficient accessible specific area of graphene also provides superb opportunity for a high loading of hemin and PEDOT in the composite matrix. Finally, the possible synergistic effect of the well-combination of three components can facilitate the electrochemical sensing performance of the nanocomposite.

2 Experimental

2.1 Reagents

Hemin (ferriprotoporphyrin Ⅸ chloride, 98 wt%) and 3,4-ethylenedioxythiophene (EDOT) were purchased from Aladdin reagents and used as received without further purification. Graphene oxide was prepared from natural graphite (12000 mesh) by a modified Hummers method we described elsewhere.[22] The real sample we used is commercially available contact lens cleaning solution (Ciba vision, Canada) containing 3% H_2O_2. Disodium hydrogen phosphate (Na_2HPO_4), sodium dihydrogen phosphate (NaH_2PO_4) and hydrogen peroxide (30%w/w) were obtained from Nanjing Chemical Regents Co., Ltd. 0.1mol L^{-1} phosphate buffer solution (PBS) was prepared from NaH_2PO_4 and Na_2HPO_4. Distilled water was used for all experiments. All other reagents were analytical grade.

2.2 Synthesis of H-GNs/PEDOT composites

Microwave synthesis of H-GNs/PEDOT composites was carried out in a CEM Discover microwave machine using single mode. Firstly, H-GNs hybrid was prepared as followed: 6.2 mg hemin was added into 4 mL homogeneous graphene oxide (GO) suspension (2.0 $mgmL^{-1}$), followed by the addition of 40μL ammonia (pH 10.0) to get a dark reddish-brown solution. The mixture was stirred mildly for overnight to allow conjugation between hemin and GO. Then, 50 mmol EDOT was inserted to the above resulting H-GNs suspension by vigorous stirring for 1.5 h. Then the resultant dispersion was transferred into a microwave vessel and fixed in the vessel holder. The maximum power setting was set as 300 W and the pressure limit was 250 psi. The microwave irradiation was set at 120 ℃ for 30 min. After the reaction completed, the microwave reaction vessel was cooled to room temperature. The black H-GNs/PEDOT composite was obtained by filtering with a nylon membrane (0.22 μm), and could be redispersed in water by ultrasonication.

2.3 Electrode modification

Prior to use, glass carbon electrode (GCE) (CH instruments, USA) with 3 mm diameter was sequentially polished with 1.0 μm, 0.3 μm, and 0.05 μm alumina/water slurry on a polishing cloth, followed by thoroughly rinsing with distilled water. After cleaning in ethanol and distilled water for 5min by ultrasonication respectively, the obtained electrode was dried with a purified N_2 stream. Typically, 5 μL 1.0 mg mL-1 H-GNs/PEDOT solution was dropped on the GCE surface and then dried at room temperature to prepare H-GNs/PEDOT/GCE.

2.4 Apparatus and measurements

Transmission electron microscopy (TEM) images were obtained with JEM-2100 (JEOL Co., Ltd., Japan). The Fourier-transform infrared spectroscopy (FT-IR) spectra were recorded with Nicolet IS-10 (Thermo Scientific Co., Ltd., USA). UV-vis absorption spectra were recorded on Evolution 220 Series UV-vis Spectrophotometer (Thermo Scientific Co., Ltd., USA).

Electrochemical measurements were carried out with a CHI660D electrochemical workstation (Shanghai Chenhua Co., Ltd., China) coupled with a traditional three-electrode system, employing a platinum wire, a saturated calomel electrode (SCE), and the bare or modified electrodes as counter, reference and working electrodes, respectively. Before experiments, the buffer solution was bubbled with pure nitrogen for about 15min for a roughly anaerobic condition. All measurements were performed at room temperature (22+0.5℃).

3 Results and discussion

3.1 Characterization of H-GNs/PEDOT film

The morphology of the as-synthesized H-GNs/PEDOT composite was characterized by TEM. From Fig.1 A, we can see that the edge of H-GNs/PEDOT film is few layers of graphene nanosheets with a typical wrinkled sheet-like feature,

and the nanosheet is almost transparent. What situated in the center section is the cascading intertwined network structure of PEDOT, implying that PEDOT has successfully grown along the graphene surface. The inset of Fig.1 A shows that nanostructured PEDOT exhibits a spindle shape with an average length of 900 nm and mid width of around 120 nm. As shown in Fig.1 B, neither individual graphene sheet nor PEDOT agglomerates can be observed, indicating the uniform growth of PEDOT with similar scale on graphene sheets. The results also indirectly demonstrate that hemin as the trigger point or catalyst of PEDOT polymerization is uniformly adsorbed on the graphene sheets.[23] The energy dispersive X-Ray spectroscopy confirmed the content of hemin is about 30 wt% (the data was not shown here).

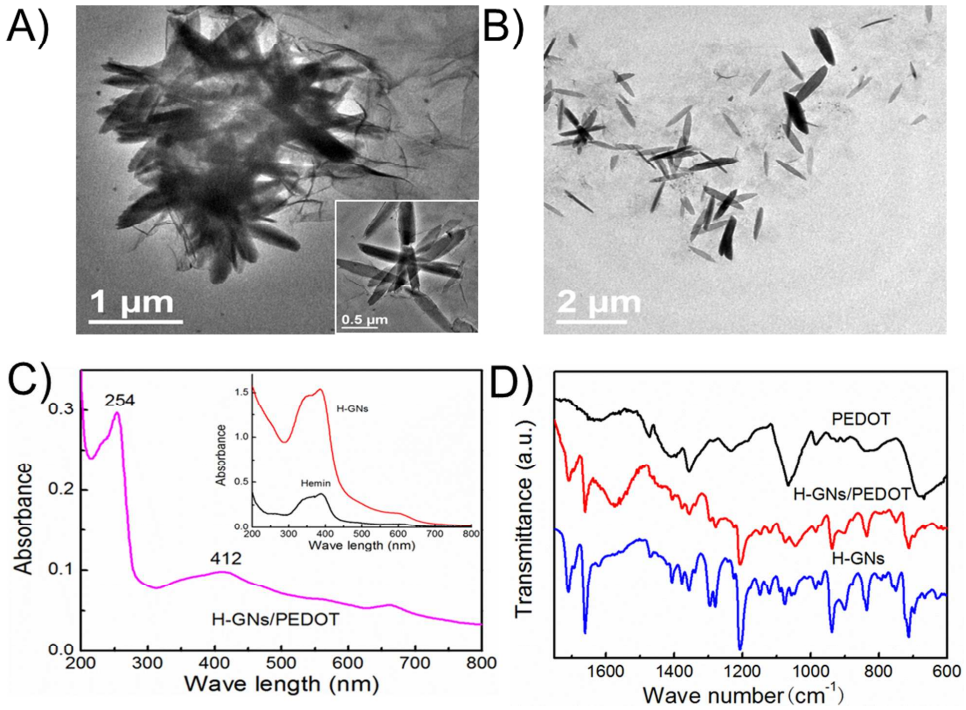

Fig.1 TEM images (A, B) of the as-synthesized H-GNs/PEDOT composite. The inset is high-magnification TEM of (A). UV-vis spectra (C) of hemin, H-GNs and H-GNs/PEDOT composite film. FTIR spectra (D) of PEDOT, H-GNs/PEDOT and H-GNs.

The evidence further demonstrating the successful synthesis of H-GNs/PEDOT was supplied by UV-vis. As shown in Fig.1 C, the spectrum of hemin ammonia solution contains a strong peak at 386 nm attributed to the Soret band, together with a group of weak peaks between 550 and 700 nm ascribed to the Q-bands. H-GNs display similar spectrum with that of hemin solution in terms of absorption band position and shape, which demonstrates the successful attachment and good bioactivity of hemin on graphene sheet.[15] It is noted that the difference of absorbance is ascribed to the different concentrations of hemin and H-GNs solution. An strong absorption at 254 nm for H-GNs/PEDOT nanocomposites is observed, which is corresponding to the chemically reduced graphene oxide,[24] and an broad absorption at ca. 412 nm with a large bathochromic shift (27 nm) can also been seen, which arises from the Soret band of hemin. These findings prove the existence of π-π interaction between graphene and porphyrin ring, and are essentially identical to the previous report.[25] The interactions of a cationic porphyrin derivation with chemically converted graphene would result in a red shift of the porphyrin Soret band.

FT-IR spectroscopy can provide some useful information on the structure of H-GNs/PEDOT composites. Fig.1 D shows the comparative IR spectra of PEDOT, H-GNs and H-GNs/PEDOT. The IR spectrum of synthesized PEDOT is roughly consistent with that reported in the literature.[20] A band at 1635 cm^{-1} and a band centered around 1352 cm^{-1} are contributed to the C=C and C-C stretching vibrations in the thiophene ring, respectively. Bands at 985, 841 and 683 cm^{-1} are assigned to the C-S bond vibration. The bands at 1228 and 1065 cm^{-1} are due to the stretching of the ethylenedioxy group. Additionally, the disappearance of a strong band at 890 cm^{-1} (the C-H bending mode of EDOT monomer) in the FTIR spectra of H-GNs/PEDOT composite further demonstrates the formation of PEDOT chains with α,α'-couplingCompared with PEDOT. H-GNs/PEDOT composite displays a bathochromic shift from 1635 cm^{-1} to 1569 cm^{-1}, which means that the conjugated PEDOT chain probably is dopped with H-GNs as the dopant. It is notable that the position and shape of vibrations for hemin in H-GNs/PEDOT are reasonable agreement with those of hemin standard spectrum and H-GNs spectrum, suggesting that hemin retains its native integrated structure and the electrocatalytic activity in the H-GNs/PEDOT composite.

Moreover, compared with the Raman spectra of single component, the broadened Raman peaks located in 1200-1600cm^{-1} of H-GNs/PEDOT also prove the combination of PEDOT with graphene sheets and hemin (demonstrated in Fig. S1†). Above all, we can conclude that the expected H-GNs/PEDOT composite has been successfully synthesized.

3.2 Direct electrochemistry of hemin on the H-GNs/PEDOT/GCE

The direct electrochemistry behavior of hemin on H-GNs/PEDOT/GCE is investigated in 5.0 mM $[Fe(CN)_6]^{3-/4-}$ containing 0.1 M KCl by Electrochemical Impedance Spectroscopy (EIS) and Cyclic Voltammetry (CV) methods.

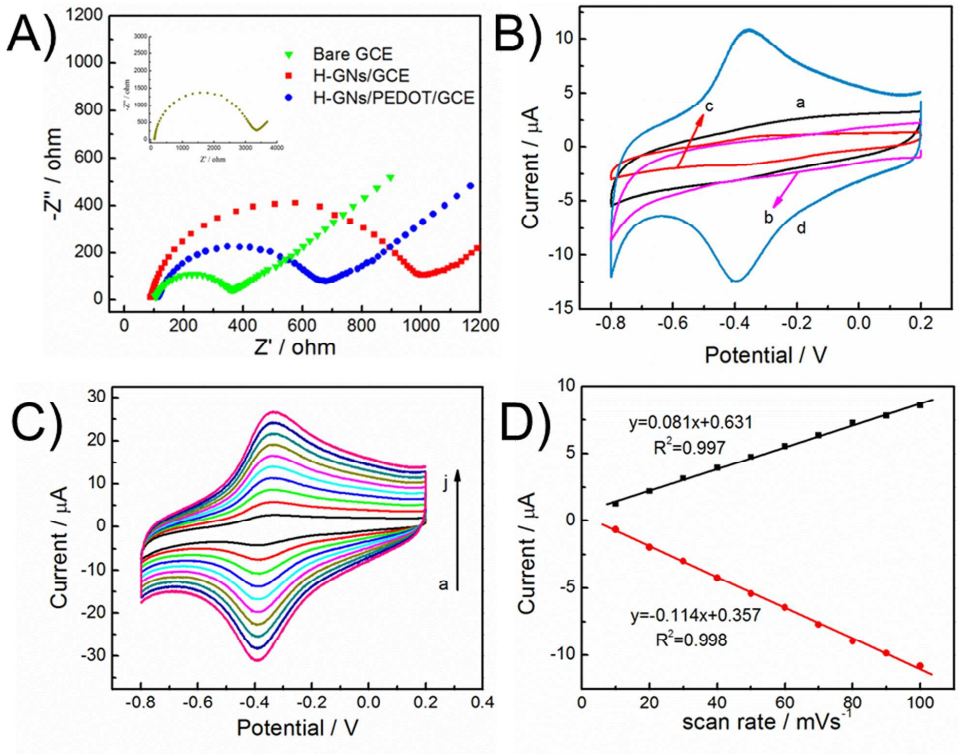

Fig.2 (A) Nyquist polts of bare GCE, H-GNs/GCE, and H-GNs/PEDOT/GCE in 5.0 mM $[Fe(CN)_6]^{3-/4-}$ containing 0.1 M KCl. Frequency range:0.1~10^6 Hz. Inset: Nyquist plot of Hemin/GCE (B) CVs of bare GCE (a), PEDOT/GCE (b), Hemin/GCE (c), and H-GNs/PEDOT/GCE (d) in 0.1M PBS. Scan rate: 100 mV s^{-1}. (C) CVs of H-GNs/PEDOT/GCE in 0.1M PBS at different scan rates (a-j) from 10 to 100 mV s^{-1}. (D) Plots of anodic and cathodic peak currents *vs.* scan rate.

As shown in Fig.2 A, the bare GCE shows a typical Nyquist plot which comprises a semicircle lying at high frequency related to the electron transfer-limited process in a film and a straight line nearly 45° at low frequency related to the diffusion-limited process. The inset of Fig.2 A shows a quite significant semicircle, which arises from the known non-conductivity of porphyrin. Compared with the plot of H-GNs/GCE, H-GNs/PEDOT/GCE exhibits a lower electron-transfer resistance (R_{et}) determined by the diameter of semicircle. It indicates that the PEDOT and graphene play important roles in accelerating the electron transfer between the electrolyte solution and electrode interface.

Fig. 2B shows the CVs of different modified electrodes in 0.1 M PBS. As expected, there were no redox peaks appearing for the bare GCE and PEDOT/GCE (curve a and b). When the bare GCE was modified with hemin, a couple of weak quasi-reversible redox peaks were seen (curve c), and the redox response is due to the single electron transfer process of iron at the inner of hemin.[15] Additionally, the background current of Hemin/GCE smaller than that of the bare GCE further demonstrated the successful immobilization of hemin. Whereas, a pair of stable and well-defined redox peaks were observed at H-GNs/PEDOT/GCE (curve d). Both the redox peaks and background current for H-GNs/PEDOT/GCE were much bigger than those for Hemin/GCE and PEDOT/GCE. The anodic and cathodic peak potentials were located at -0.357 and -0.410 V, respectively, which resulted from direct electron transfer of the immobilized hemin for the conversion between Fe(III) and Fe(Ⅱ). The peak-to-peak potential separation (ΔE_p) was 53 mV at a scan rate of 100 mV s^{-1}, much smaller than some other hemin modified electrodes reported,[26, 27] implying a fast direct electron-transfer between the redox-active site of hemin and the modified electrode. Apparently, the presence and good synergy effect of graphene and PEDOT are decisive factors for the achievement of rapid electron transfer of hemin.

CVs of H-GNs/PEDOT film modified electrode at various scan rate are shown in Fig.2C. The redox peak currents corresponding to hemin increased as a function of scan rate. The cathodic and anodic peak currents increased linearly with the scan rate from 10 to 100 mV s^{-1}, indicating that hemin embedded in H-GNs/PEDOT film underwent a surface-

controlled process. For such a surface process, the surface concentration (Γ*) can be estimated by the Laviron equation:[28]

$$I_p = \frac{n^2F^2vI^{*}A}{4RT}$$

Where I_p is the peak current, n is the number of electron(s) transferred (n=1), F is the Faraday constant, v is the scan rate, A is the effective surface area (0.072 cm^2), R is the gas constant, and T is the temperature (298.15K). According to the slop of I_p *vs* v, the surface concentration is calculated to be 1.22×10^{-9} mol cm^{-2}, which is larger than the theoretical monolayer coverage of hemin (6.89×10^{-11} mol cm^{-2}). It means that the surface area of H-GNs/PEDOT film is efficiently enlarged through combination of graphene and PEDOT chains to provide a cross linked network structure for better loading of hemin and the analytes,[29] which can enhance the catalytic ability and faradic response.

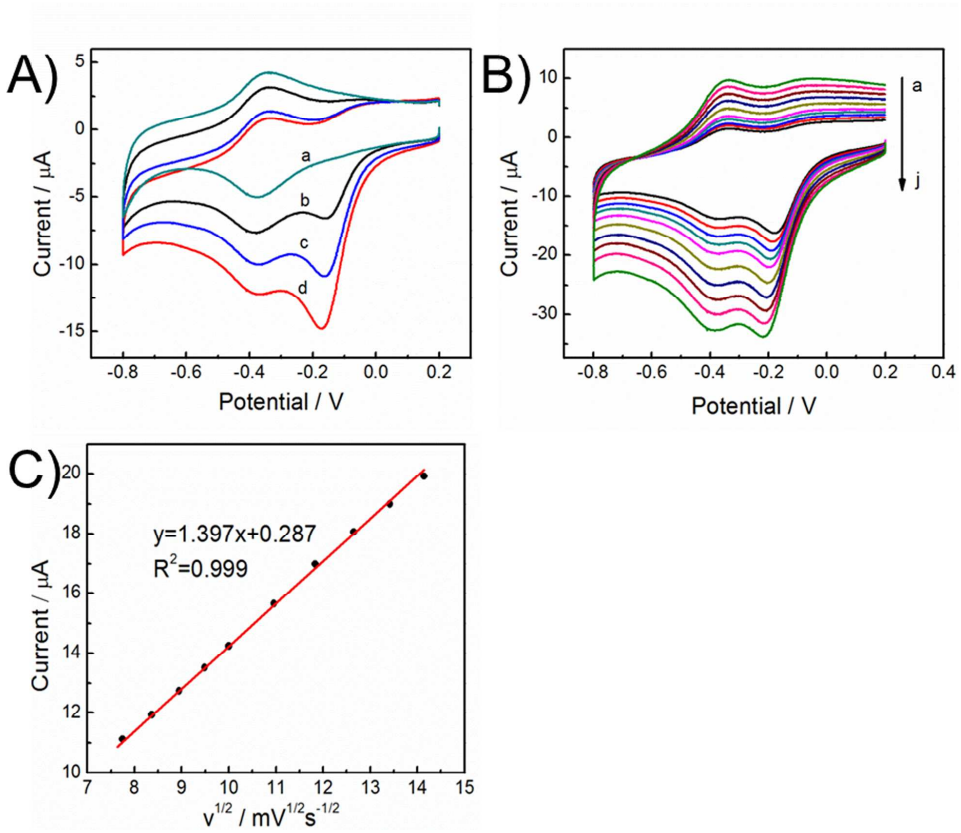

Fig.3 A) CVs of H-GNs/PEDOT/GCE in 0.1 M PBS (pH 7.0) containing (a) 0, (b) 0.5, (c) 1.0, (d) 1.5 mM H_2O_2, respectively. Scan rate: 50 mV s^{-1}. B) CVs of H-GNs/PEDOT/GCE in the presence of 1.5 mM H_2O_2 at varying scan rates from 60 to 200 mV s^{-1}. C) The plot of cathodic peak currents vs. $v^{1/2}$.

3.3 Electrocatalysis of H-GNs/PEDOT film towards H_2O_2

To investigate the electrocatalytic activity of H-GNs/PEDOT/GCE towards H_2O_2, CV was employed over a potential range from -0.8 to 0.2V. Fig.3 A shows CVs of H-GNs/PEDOT/GCE in 0.1 M PBS (pH7.0) in the presence of different concentrations of H_2O_2. Clearly, CV of H-GNs/PEDOT/GCE only shows characteristic redox peak of hemin without H_2O_2. Upon addition of 0.5 mM H_2O_2, a new well-defined reduction peak centered at -0.162V appears. Further increasing the concentration of H_2O_2 from 0.5 to 1.5 mM, the corresponding cathodic peak current increased progressively, indicating the occurrence of typical electrocatalytic reduction process of H_2O_2. It is worth noting that the reduction potential of H_2O_2 is significantly lower than the values reported in literature.[7, 9, 29] The low operation potential enables the H_2O_2 biosensor with a better sensitivity since it gives less exposure to interfering reactions, which is different from the redox mediators based ones.[30] The reduction of H_2O_2 results from the electrocatalysis process of $hemin_{red}$, while $hemin_{red}$ itself is oxidized to $hemin_{ox}$ and then quickly reduced back to $hemin_{red}$ through its direct electron transfer with the electrode.[4]

Fig. 3B shows the CVs of H-GNs/PEDOT/GCE recorded in 0.1 M PBS in the presence of 1.5 mM H_2O_2 at different scan rates. Obviously, the reduction peak current of H_2O_2 increases linearly with the square root of the scan rate in the range 60-200 mV s^{-1} (Fig. 3C), indicating a diffusion-controlled process of H_2O_2.

Journal Name

RSCPublishing

ARTICLE

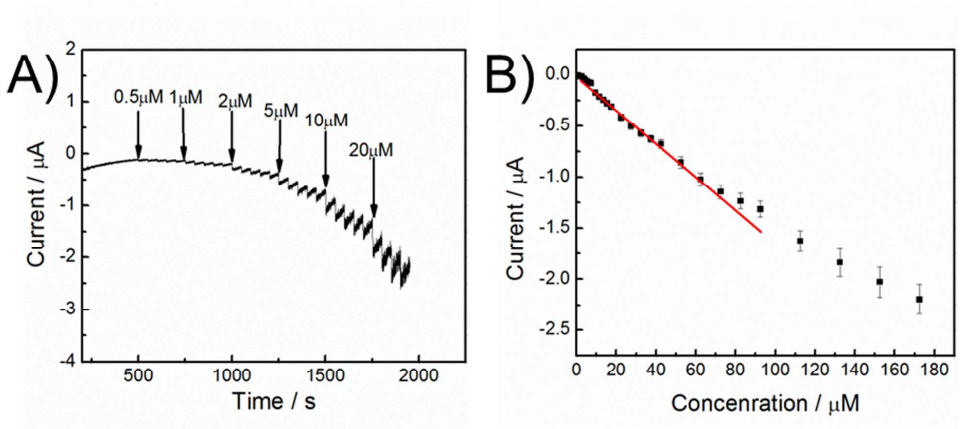

Fig.4 A) Amperometric response of H-GNs/PEDOT/GCE upon the successive addition of H_2O_2 at low concentrations (0.5, 1, 2, 5, 10, 20 μM) into a gently stirred 0.1 M PBS. Applied potential: -0.2 V. B) The plot of electrocatalytic current of H_2O_2 vs. the corresponding concentration. Error bars indicate standard deviations for three independent measurements at each H_2O_2 concentration.

As previously mentioned, accurate and fast detection of H_2O_2 is of extremely importance. Herein, the determination of H_2O_2 on H-GNs/PEDOT/GCE was investigated using amperometric method. Fig.4 A shows a typical amperometric response of the H-GNs/PEDOT/GCE upon successive addition of a certain concentration of H_2O_2 into stirred 0.1M phosphate buffer solution (pH 7.0) at regular intervals of 50s. The applied potential (E_{app}) was hold at -0.2V *vs.* SCE. For every addition of H_2O_2, a well-defined and stable amperometric response was observed immediately, and achieved 95% steady-state current towards H_2O_2 within 3s, indicating that the electrocatalytic reaction was sensitive and extraordinarily rapid. The response currents were increased linearly with the concentration of H_2O_2 from 0.5 μM to 70 μM. The calibration curve for the H-GNs/PEDOT/GCE is shown in Fig. 4 B. The linear regression equation expressed as I_p /μA = -0.0167×[H_2O_2]/μM+0.00147 (R^2=0.985). The sensitivity was calculated to be 235 μA$mM^{-1}cm^{-2}$.[31-33] The limit of detection (LOD) could reach as low as 0.08 μM based on the formula LOD =3S_b/S (where, S_b =standard deviation of blank signal and S =sensitivity).[7] The analytical performance of the proposed biosensor towards determination of H_2O_2 is superior over some other reported heme related sensors in terms of wide linear range, high sensitivity and low LOD.[16, 32-34]

Selectivity of the obtained biosensor towards H_2O_2 was investigated with the interference of some common substances such as dopamine, uric acid, ascorbic acid and glucose. Fig.5 represents the amperometric response for successive addition of 1 μM H_2O_2 and 10-fold concentration of dopamine (DA), uric acid (UA), ascorbic acid (AA), glucose and 1 μM H_2O_2 at the H-GNs/PEDOT/GCE. A stead-state amperometric response was observed towards 1 μM H_2O_2, whereas no obvious responses, generally less than 2%, were obtained for the sequentially addition of above-mentioned interfering species. Again well-defined amperometric response was also obtained with subsequent addition of 1 μM H_2O_2 into the above buffer solution. Thus selective determination of H_2O_2 can be achieved even in the coexistence of high concentrations of common interfering species, revealing the excellent selectivity of the as-proposed biosensor based on H-GNs/PEDOT/GCE.

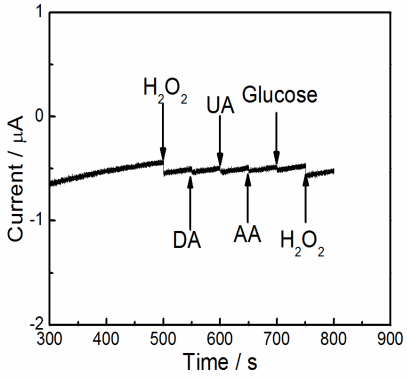

Fig.5 Amperometric response of H-GNs/PEDOT/GCE at -0.2 V for the sequential addition of 1 μM H_2O_2, 10 μM DA, 10 μM UA and 10 μM AA, 10 μM glucose and 1 μM H_2O_2.

The reproducibility, stability and repeatability of the sensor were also evaluated. Only a slight decrease of peak currents about 7% could be seen from CV curves after 100

cyclic scans in pH 7.0 PBS at 100 mV s^{-1}. When the electrode was stored at 4℃ and measured after three weeks, the current response corresponding to hemin redox reaction only showed a 15% decrease of the original value, indicating a good stability. The relative standard deviation (RSD) of the peak current in six successive determinations at a H_2O_2 concentration of 0.5 mM was 5.6% for H-GNs/PEDOT/GCE. The good stability might be attributed to the good biocompatibility of the well-combined composite, to the synergistic effect and the unique properties of the three components. Five different modified GCEs were independently fabricated (using the same GC electrode), the peak current related to the redox reaction of hemin was tested by CV, and the corresponding RSD value determined was less than 5%. The repeatability of the modified electrodes was also acceptable.

To investigate the practical feasibility of the H-GNs/PEDOT/GCE biosensor, the commercially available contact lens cleaning solution containing 3% H_2O_2 was examined. The real sample was diluted with PBS (pH 7.0) to obtain the required H_2O_2 concentration shown in the Table 1, and the amperometric experiment was performed with experimental conditions similar to lab sample. The real sample results for contact lens cleaning solution (using standard addition method) are listed in Table 1.

Table 1 The recovery determination of H_2O_2 in contact lens cleaning solution sample.

Added (mM)	Real sample Found (mM)		Recovery (%)
	Mean[a]	R.S.D[b] (%)	
4.9	4.96	8.8	101.2
9.8	9.51	7.7	97.0
19.6	19.71	3.7	100.6
29.4	29.73	3.2	101.1
53.9	53.79	3.1	99.8

[a] Average of three determinations.

[b] Relative standard deviation.

Conclusions

The H-GNs/PEDOT nanocomposite was facilely synthesized via microwave-assistant method and its biomimetic sensing to H_2O_2 was also investigated. We have described the fabrication a novel H_2O_2 biosensor consisting of H-GNs/PEDOT composite film. The high performance of H-GNs/PEDOT modified GCE showed that PEDOT and graphene have an excellent synergic effect with hemin in stimulating the electron transfer of hemin. Moreover, the hemin embedded in the composite film maintained good electrocatalytic activity towards hydrogen peroxide. The results of electrochemical detection of H_2O_2 indicate H-GNs/PEDOT/GCE exhibits high sensitivity and low detection limit towards the reduction of H_2O_2 compared with other related hemin based sensors reported in the literature. Additionally, the low cost, very fast response time, good stability, repeatability and selectivity of the H-GNs/PEDOT modified electrode make it a potential candidate for the fabrication of novel H_2O_2 biosensors. Moreover, in comparison to other nanomaterials, the environment friendly, cost-efficient and large production of H-GNs/PEDOT fabricated through microwave approach also makes it a promising material for other biosensors.

Acknowledgements

The work was supported by the National Natural Science Foundation of China (No. 21103092), Program for NCET-12-0629, the Fundamental Research Funds for the Central Universities (No. 30920130111003), the Ph.D. Programs Foundation of Ministry of Education of China (No.20133219110018), Qing Lan Project and Six Major Talent Summit (XNY-011), the Science and Technology Support Plan and PAPD of Jiangsu Province, China (Nos.BE2011835 and BE2013126).

Notes and references

[a] *School of Chemical Engineering, Nanjing University of Science and Technology, Nanjing, 210094, China. Tel.: +86-25-84315943; Fax: +86-25-84315190;E-mail: qinglihao@njust.edu.cn; haoqingli@yahoo.com (Q. Hao)*

1. R. M. Santos, M. S. Rodrigues, J. Laranjinha and R. M. Barbosa, *Biosensors & bioelectronics*, 2013, **44**, 152-159.
2. S. Peteu, P. Peiris, E. Gebremichael and M. Bayachou, *Biosensors & bioelectronics*, 2010, **25**, 1914-1921.
3. Z.-X. Liang, H.-Y. Song and S.-J. Liao, *The Journal of Physical Chemistry C*, 2011, **115**, 2604-2610.
4. H. Song, Y. Ni and S. Kokot, *Analytica chimica acta*, 2013, **788**, 24-31.
5. L. Fruk and C. M. Niemeyer, *Angewandte Chemie*, 2005, **44**, 2603-2606.
6. A. Durkop and O. S. Wolfbeis, *Journal of fluorescence*, 2005, **15**, 755-761.
7. V. Mani, B. Dinesh, S. M. Chen and R. Saraswathi, *Biosensors & bioelectronics*, 2014, **53**, 420-427.
8. M. M. Barsan, E. M. Pinto and C. M. A. Brett, *Electrochimica Acta*, 2010, **55**, 6358-6366.
9. C. Guo, F. Hu, C. M. Li and P. K. Shen, *Biosensors & bioelectronics*, 2008, **24**, 825-830.
10. W. Sun, L. Cao, Y. Deng, S. Gong, F. Shi, G. Li and Z. Sun, *Analytica chimica acta*, 2013, **781**, 41-47.
11. X. He, L. Zhou, E. P. Nesterenko, P. N. Nesterenko, B. Paull, J. O. Omamogho, J. D. Glennon and J. H. Luong, *Analytical chemistry*, 2012, **84**, 2351-2357.
12. C. Zhao, L. Wan, L. Jiang, Q. Wang and K. Jiao, *Analytical biochemistry*, 2008, **383**, 25-30.
13. M. Zhou, Y. Zhai and S. Dong, *Analytical chemistry*, 2009, **81**, 5603-5613.
14. Y. Xu, Z. Liu, X. Zhang, Y. Wang, J. Tian, Y. Huang, Y. Ma, X. Zhang and Y. Chen, *Advanced Materials*, 2009, **21**, 1275-1279.
15. Y. Guo, L. Deng, J. Li, S. Guo, E. Wang and S. Dong, *ACS nano*, 2011, **5**, 1282-1290.

16. J. Chen, L. Zhao, H. Bai and G. Shi, *Journal of Electroanalytical Chemistry*, 2011, **657**, 34-38.
17. Y. Guo, J. Li and S. Dong, *Sensors and Actuators B: Chemical*, 2011, **160**, 295-300.
18. Y. Zhou, M. Wang, X. Meng, H. Yin and S. Ai, *RSC Advances*, 2012, **2**, 7140.
19. W. Si, W. Lei, Y. Zhang, M. Xia, F. Wang and Q. Hao, *Electrochimica Acta*, 2012, **85**, 295-301.
20. S. V. Selvaganesh, J. Mathiyarasu, K. L. N. Phani and V. Yegnaraman, *Nanoscale Research Letters*, 2007, **2**, 546-549.
21. L. C. Chang, H. N. Wu, C. Y. Lin, Y. H. Lai, C. W. Hu and K. C. Ho, *Nanoscale Res Lett*, 2012, **7**, 319.
22. H. Wang, Q. Hao, X. Yang, L. Lu and X. Wang, *Nanoscale*, 2010, **2**, 2164-2170.
23. Q. Sheng, M. Wang and J. Zheng, *Sensors and Actuators B: Chemical*, 2011, **160**, 1070-1077.
24. J. Zhang, H. Yang, G. Shen, P. Cheng, J. Zhang and S. Guo, *Chemical communications*, 2010, **46**, 1112-1114.
25. Y. Xu, L. Zhao, H. Bai, W. Hong, C. Li and G. Shi, *Journal of the American Chemical Society*, 2009, **131**, 13490-13497.
26. J. Wei, J. Qiu, L. Li, L. Ren, X. Zhang, J. Chaudhuri and S. Wang, *Nanotechnology*, 2012, **23**, 335707.
27. Q. Ma, S. Ai, H. Yin, Q. Chen and T. Tang, *Electrochimica Acta*, 2010, **55**, 6687-6694.
28. E. Laviron, *Journal of Electroanalytical Chemistry and Interfacial Electrochemistry*, 1979, **100**, 263-270.
29. G. Ran, W. J. Yi, Y. Li, H. Q. Luo and N. B. Li, *Analytical Methods*, 2012, **4**, 2929.
30. W. Chen, S. Cai, Q. Q. Ren, W. Wen and Y. D. Zhao, *The Analyst*, 2012, **137**, 49-58.
31. S. Woo, Y.-R. Kim, T. D. Chung, Y. Piao and H. Kim, *Electrochimica Acta*, 2012, **59**, 509-514.
32. M.-Y. Hua, Y.-C. Lin, R.-Y. Tsai, H.-C. Chen and Y.-C. Liu, *Electrochimica Acta*, 2011, **56**, 9488-9495.
33. K.-P. Lee, A. I. Gopalan and S. Komathi, *Sensors and Actuators B: Chemical*, 2009, **141**, 518-525.
34. X. Che, R. Yuan, Y. Chai, L. Ma, W. Li and J. Li, *Microchimica Acta*, 2009, **167**, 159-165.

Journal Name

RSCPublishing

ARTICLE

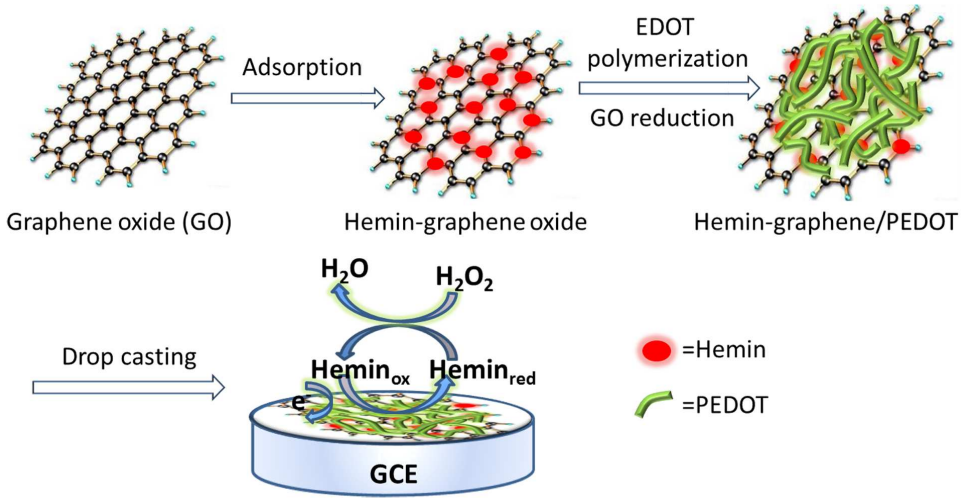

The ternary nanocomposite hemin-graphene sheets / poly (3,4-ethylenedioxythiophene) (H-GNs/PEDOT) synthesized by the microwave - assistant method exhibits good electrocatalytic activity towards the reduction of hydrogen peroxide.